INTERNATIONAL JOURNAL OF AUTOMOTIVE AND MECHANICAL ENGINEERING
ISSN: 2229-8649 e-ISSN: 2180-1606
VOL. 20, ISSUE 2, 2023, 10536 – 10546
DOI: https://doi.org/10.15282/ijame.20.2.2023.15.0813

RESEARCH ARTICLE

Development of Empirical Model for Electromagnetic Damping Coefficient Damper

M.F. Mohd Yusoff[1,*], A.M. Ahmad Zaidi[2], S.A. Firdaus Ishak[1], M.K. Awang[1], M.F Md Din[1], A. Mukhtaruddin[1], Muhammad Haikal Aiman Jefri[1], Tan Kean Sheng[1] and Azharudin Mukhtaruddin[1]

[1]Faculty of Engineering, National Defence University of Malaysia, 57000 Kuala Lumpur, Malaysia
[2]Faculty of Defence Science and Technology, National Defence University of Malaysia, 57000 Kuala Lumpur, Malaysia

ABSTRACT - The significance of the electromagnetic damper in vibration systems has attracted considerable interest from researchers, making it a prominent area of research. Various papers have been consulted to explore the vibration concept associated with electromagnetic dampers and their practical applications. A vibration test rig with a simple electromagnetic damper has been designed and tested to investigate the effect of electromagnetic force. An experimental study on the response of the electromagnetic damper was conducted. A logarithmic decrement method was deployed to find the damping coefficient, c, of a one-degree freedom system (mass spring damper system). A test rig and electromagnetic damper element were introduced as a damper in the system. Design factors included the type of geometry, type of material and the current supply to the system. The testing was conducted using the in-house developed vibration test rig. The data obtained from the experiment has been analysed to determine the electromagnetic damping performance. A factorial analysis was performed to identify the significant factors influencing the damping coefficient of the system. Two empirical models obtained through regression analysis of Excel and Minitab. It was found that the influential effects for the response are the type of material (aluminum), slotted geometry and a bigger amount of current (3 A). The application of a cylindrical conductor and magnet as a damper reduced the vibration response of spring mass damper.

ARTICLE HISTORY
Received : 15th Nov 2022
Revised : 08th June 2023
Accepted : 26th June 2023
Published : 03rd Aug 2023

KEYWORDS
Electromagnetic damper;
Vibration;
Empirical model;
Eddy current

1.0 INTRODUCTION

Vibration and damping are two main research areas that are related very closely. Vibration can be useful as well as vulnerable to a system or machines. An engineer in this field is tasked with addressing problems and challenges related to mechanical systems, including issues such as fatigue, fracture, and energy loss. These matters are crucial focal points requiring attention and resolution. Engineers are combatting those issues by keeping on improving vibration damping and /or isolation techniques. Mechanical vibration problems are common in industrial, transportation, and defence application. Vibration rapidly can cause problems for the user and also for the system. By the literatures review, conventional damper have few deficiencies, which are conventional damping reduces the life cycle of the machine due to the unwanted vibration in the damping system and less efficiency in reducing vibration. Other than that, some researchers found that the damping action of a viscous damper decrease at resonance condition, while the electromagnetic damper has no effect on resonance.

The electromagnetic damper is an alternative to the traditional passive system-based conventional dampening technology[1]. An electromagnetic damper is another method to create damping in any vibration system. There are now several dampening devices that operate based on the electromagnetism concept[2] [3][4][5][6][7][8]. Song C. L. et al.[9], conducted an electromagnetic application study, utilising a permanent magnet as a plunger to achieve rectilinear and turning motions in a multi-segmented robot. The coil surrounding the permanent magnet was energised by a current, which in turn generated an actuation force based on the Biot-Savart law. The Biot-Savart law expresses the magnetic field along the axis of a circular current loop with radius r and steady current i as follows:

$$B_{sol} = \frac{\mu_0}{4\pi} \int \frac{dl \times r'}{|r'|^3} \tag{1}$$

where dl and r' are the line segment and distance vector from the viewpoint of the source charge. Figure 1 elucidates the schematic diagram of the phenomenon which contributes to the electromagnetic force as:

$$\boldsymbol{F_z(z,i)} = \int \sigma_m \boldsymbol{B_{sol,z}} ds = \frac{B_r}{\mu_0} \boldsymbol{B_{sol,z}} \int_0^{2\pi} \int_0^{\frac{d}{2}+\alpha} r \, dr \, d\varphi = \frac{B_r B_{sol.z} A}{\mu_0} \hat{z} \, . \tag{1}$$

*CORRESPONDING AUTHOR | Mohd Fazli bin Mohd Yusoff| ✉ fazli@upnm.edu.my

From this equation, it is clearly shown that the force that occurs in the system originated from the magnetic flux density from the magnet and the induction coil with respect to the area and permeability of the cylinder surrounding it.

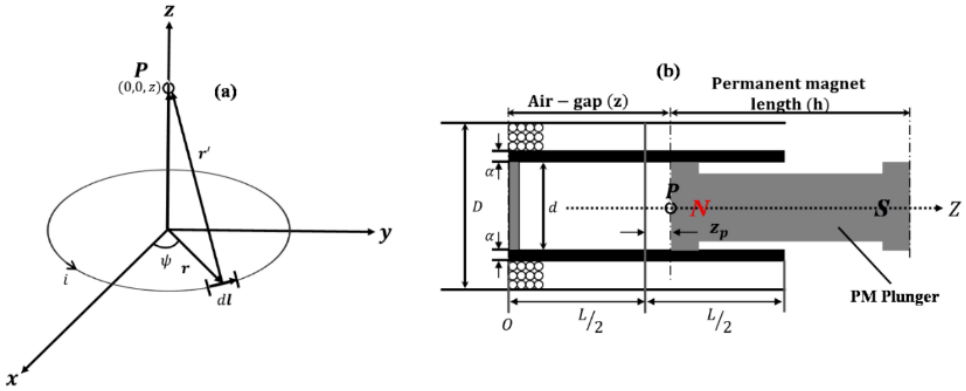

Figure 1. (a) Schematic diagram of a coil induced by current i; (b) the cross-section of a solenoid featuring a permanent magnet (PM) plunger, along with the associated design parameters [9]

Another application of electromagnetic damper was applied to a cable structure [2]. The relative motion between the coil and the permanent magnet gives rise to an electromagnetic force that can be utilised to regulate the vibration of a structure. The electromagnetic (EM) damper, serving both as a vibration-control device and an energy-harvesting mechanism, has emerged as a promising maintenance approach for cable structures. By positioning a permanent magnet within a coil, an induction current is induced, resulting in the generation of the Lorentz force[2]. This Lorentz force, acting as the damping force of the damper, operates in opposition to the permanent magnet.

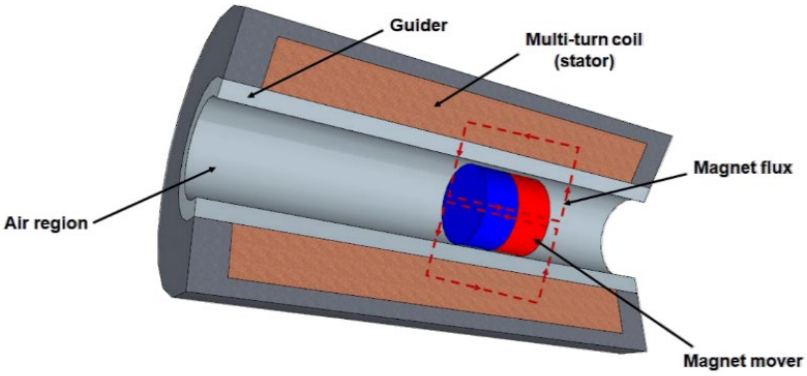

Figure 2. Configuration of electromagnetic damper [2]

Electromagnetic damping is the focus of continuous study and development. In 2018, Jamshidi et al. emphasised that an electromagnetic damper possesses the advantage of not requiring additional power to generate the damping force. They further highlighted that the equivalent damping of the damper could be adjusted effectively by utilising a simple switched circuit. [10]. A hybrid electromagnetic damper prototype was developed, and the characterisation of the damper was analysed experimentally. The term hybrid in this context denotes the combination of passive and semi-active modes within the system. The passive mode serves as a harvester, collecting energy, while the semi-active mode is an energy supplier for the sensors and microcontroller. The harvested energy is utilised to power these components. The linear electromagnetic motor has been used as the core part to generate the voltage from the linear movement of the system[11][12].

In a recent paper by Kong et al. [6], the electromagnetic effect was employed as a means to control the position of a permanent magnet. By utilising the induced magnetic field generated by an electromagnetic coil, the suspended magnet is stabilised in the vertical direction, while the annular permanent magnet controls the force in the horizontal direction, as illustrated in Figure 3. The movement of the base, connected to a Hall effect sensor, generates a corresponding current that is supplied to the coil. The acceleration of the measured object can be calculated based on the displacement of the suspended magnet, which is detected by the Hall sensor.

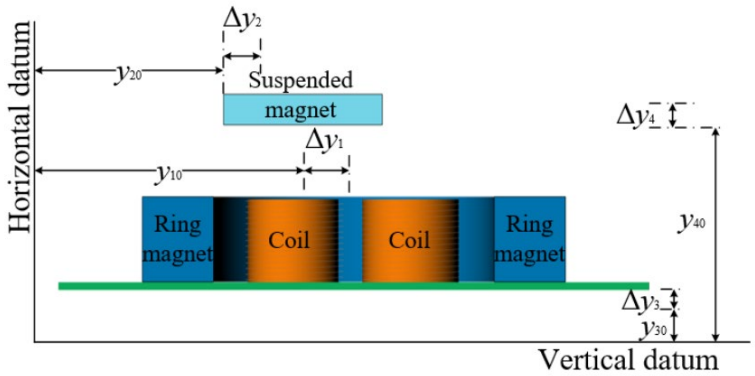

Figure 3. Measuring schematic diagram for electromagnetic suspension acceleration [6]

An application of electromagnetic damping force in a balancing-type scale was made using an electromagnetic force compensation (EMFC), as shown in Figure 4. As the beam displaced due to the weight of an unknown mass, an induced current was induced in the conductor (bobbin), which created a magnetic field that will interact with the magnetic field from the permanent magnet. Thus, a dampening effect occurs as the magnetic field induced will try to oppose the motion through which it is induced.

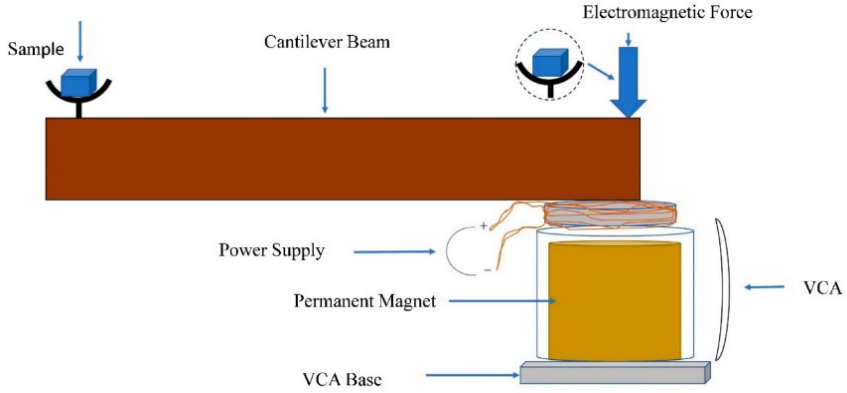

Figure 4. Application of electromagnetic damping force to balance a cantilever beam [8]

Recently the discovery of one of the simplest electromagnetic damping systems was made by [13], which consists of a magnet and a conductor tube to generate an electromagnetic field. The magnetic force between the magnet and conductor can be used to absorb shocks created due to various factors, such as uneven road conditions. The basic idea of this research is to create a magnetic flux interaction between the permanent magnet and the hollow cylinder which surrounds the permanent magnet movement. The permanent magnet moves vertically through the electromagnetic damper (a coil wounded a hollow cylinder), as shown in Figure 5. A power supply was connected to the coil such that the cylinder would react as a solenoid.

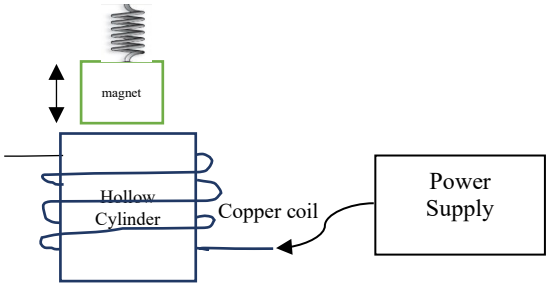

Figure 5. Schematic diagram of the main effect occurs

The electromagnets of solenoid are created by wrapping wire around any electrically conducting metal. Using the righthand rule, the direction of the magnetic field created by a current-carrying broken wire may be determined. The magnetic flux density in areas perpendicular to the magnetic field is measured in Tesla units [14]. In a study that being conducted by [15], they stated that a solenoid is insulated copper wire wound in a plastic tube or cylindrical carton that is longer than its diameter and acts as a magnet when a current is generated to pass through it. The configuration of the magnetic field lines across a current-carrying solenoid is the same as the pattern of a bar magnet shown in Figure 5. Within a solenoid, the magnetic field exhibits uniformity. As per the Right-Hand Rule theory, the end of the solenoid where the current flows in an anticlockwise direction are regarded as the north pole, while the end where the current flows in a clockwise direction are identified as the south pole.

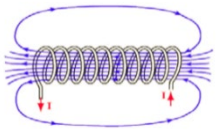

Figure 6. Magnetic field in a solenoid [15]

From Figure 6, the magnetic field in the middle of a long solenoid is concentrated into an almost uniform field. Equation 1 below shows the equation of the magnetic field [16]:

$$B = \mu_0 nI \tag{1}$$

where, B = magnetic field, μ = permeability, n = turn density, I = current passing through the wire and $\mu_0 = 4\pi \times 10^{-7}$

For the turn density,

$$n = \frac{N}{L} \tag{2}$$

where, N = number of turns, L = length of the solenoid.

Faraday's induction principle states that when a magnetic bar is inserted into a cylindrical coil (solenoid), it induces the generation of electromagnetic flux within the coil. As a result, the solenoid becomes operational and exhibits its intended functionality [8],[17],[18]. The voltage produced in a single turn of wire wrapped around a magnetic core is equal to the rate of change of the magnetic flux enclosing that wire. Lenz's law says that when an EMF is formed by a change in magnetic flux in accordance with Faraday's Law, the polarity of the induced EMF is such that it induces a current with a magnetic field that opposes the field that was initially changing [19]. This is the same concept applied in [9], where a solenoid has been activated by supplying a current to the coil such that the magnetic flux from the permanent magnet and solenoid will interact. Previously the author has simulated the electromagnetic damper using Finite Element Magnetic Method (FEMM) to see how does magnetic flux changing with several variations of parameters (material, dimension and current) [20].

In this paper, the research has been extended such that the performance of electromagnetic damper in a spring mass damper system can be studied and analysed. The damping coefficient, c, from the mass spring damper system has been extracted through the experimental system before being calculated using the logarithmic decrement method. Thus, a novelty of the research was being able to relate the vibration response of the system with the damping coefficient, c, of the electromagnetic damper. The response was then further analyse using Minitab such that the most effected parameters of the system can be identified.

2.0 METHODOLOGY

Experimental verification has been conducted in this study to emphasise the impact of the electromagnetic damper within a mass spring damper system. A logarithmic decrement method was deployed to find the damping coefficient of the overall system. Several parameters of electromagnetic dampers, such as current existence, the design's geometry of the conductor tube and the material used to fabricate the tube conductor, had been varied to find the best damping coefficient.

2.1 Damping Ratio ζ Calculation through Vibration Response

The damping ratio ζ is a dimensionless quantity that characterises the decay of oscillations in a system following a disturbance. It represents the rate at which oscillations diminish from one bounce to the next. The damping ratio ζ is a measurement describing how rapidly the oscillations decay from one bounce to the next. The damping ratio is a system parameter that can take on various values: undamped ($\zeta = 0$), underdamped ($\zeta < 1$), critically damped ($\zeta = 1$) or overdamped ($\zeta > 1$). In this experiment, the damping ratio was determined through logarithmic decrement due to the system being underdamped.

The period of oscillation, denoted as T, represents the time interval between two peaks and can be computed as [13],

$$T = \frac{t_n - t_0}{n} \tag{3}$$

here t_n refers to the time at which the n^{th} peak is observed, as depicted in Figure 7,

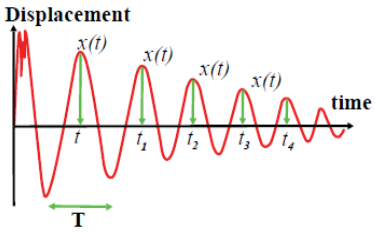

Figure 7. Oscillation response for a typical free damped vibration system [13]

The logarithmic decrement can be defined as follows [21].

$$\delta = \log\left(\frac{x(t_n)}{x(t_{n+1})}\right) \tag{4}$$

where $x(t_n)$ is a displacement located at the n^{th} peak.

From T and δ in Eq. (3) and (4), the damping ratio, ζ, can be calculated as follows.

$$\zeta = \frac{\delta}{\sqrt{4\pi^2 + \delta^2}} \tag{5}$$

2.2 *Damping Coefficient, c*

The damping coefficient, c, is the main effect that is being investigated in this research. The system's damping coefficient is a measurement of how quickly the system oscillation returns to rest as the frictional force dissipates its oscillation energy. The damping coefficient can be calculated by obtaining the values of the damping ratio, mass of sprung mass and spring stiffness of the system. From the damping ratio, ζ in Eq. (9), the value of damping constant, c, affected the value of damping ratio, ζ, according to the equation below.

$$\xi = \frac{\delta}{\sqrt{(4\pi)^2 + \delta^2}} = \frac{c}{2\sqrt{mk}} \tag{6}$$

where, *m*=mass, *k*= spring stiffness and *c*= damping coefficient.

2.3 *Experimental Setup of Electromagnetic Damper*

The experimental setup consists of sensors (accelerometers), LMS Scadas Mobile measurement hardware, and a computer with the installed software, as shown in Figure 8. LMS TestXpress software has been used to connect the LMS Scadas Mobile with the accelerometer. The accelerometer extracts the response of the system, which then converts to velocity as well as displacement response. AutoCAD was employed to create a detailed representation of the experimental test rig system, allowing the components to be visually displayed with clarity, as illustrated in Figure 9.

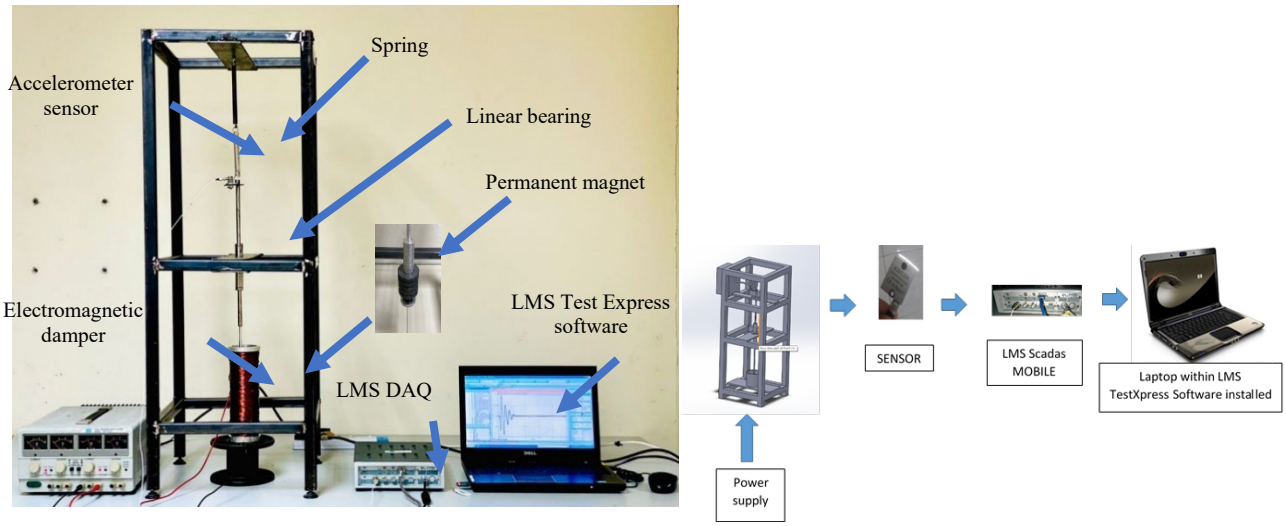

Figure 8. Overall vibration test rig system

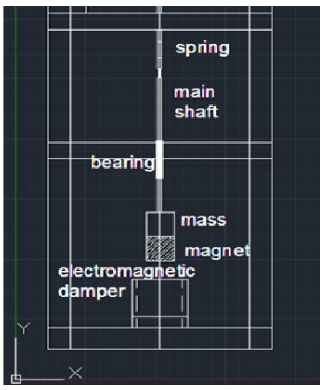

Figure 9. Main component of the vibration test rig

The test rig was built using an iron rod with a dimension of 320×320×980 mm (length×width×height). The spring stiffness, k, is 1.09 N/cm. A hollow ferrite cylindrical type of permanent magnet has been chosen with the parameters as follows.

Inner diameter	: 22 mm
Outer diameter	: 45 mm
Thickness of the magnet	: 8 mm
Pole piece to stack the magnet	: 2 mm

A linear bearing was used in the middle of the test rig to make sure the vertical movement is smooth during vibration. The experiment was carried out on two different materials for cylindrical conducting tubes, namely nylon and aluminium. Two different designs of conductor are with slotted and non-slotted dimensions with different excitation of input current. Figure 10 shows the conductor tube that is used as the electromagnetic damper.

Figure 10. Cylindrical tube with copper coil winding

The electromagnetic damper was built from two cylindrical conducting tube (aluminum and nylon) with copper winding coil surrounding it. The diameter of the copper wire was 0.5 mm. The parameters of the electromagnetic damper can be seen in Table 1.

Table 1. Parameters of the electromagnetic damper

Type of dimension	Value (m)
Length of material with winding coil (aluminum and nylon), l	0.220
Inner diameter of material (aluminum and nylon), d	0.066
Outer diameter of slotted material (aluminum and nylon), d	0.076
Thickness of material (aluminum and nylon), l	0.005
Length of permanent magnet, l	0.060
Diameter of permanent magnet, d	0.045
Gaps between magnet and material, l	0.011

3.0 EXPERIMENTAL RESULTS

Initially, the value of the magnetic damper for different configuration settings in static was measured, and the data were tabulated in Table 2. For a better understanding of the effect due to the material, current supplied and geometry design several bar charts were plotted. Next, each configuration of the electromagnetic damper was tested using the 1DOF vibration test rig, and the best damper configuration was selected by comparing the experimental damping coefficient. The damping coefficient, Cd, has been obtained from the experimental response using the logarithmic decrement method (equation 4). Then, the damping coefficient Cd has been calculated using Eq. (5) and Eq. (6). Below is the result obtained from the experimental and the calculated value of the damping coefficient being tabulated in Table 3. Figure 12(a) and 12(b) show the results obtained from the experimental test for aluminium with slotted and non-slotted configurations.

Table 2. Value of magnetic flux density of each configuration of damper obtained from static measurement

Configuration of electromagnetic damper -Material (Current, design)	Magnetic flux Density (T)			Average magnetic Flux Density (T)
	Top	Middle	Bottom	
Aluminum (1A, Not slotted)	0.0035	0.0103	0.0030	0.0056
Aluminum (3A, Not slotted)	0.0062	0.0139	0.0060	0.0087
Aluminum (1A, slotted)	0.0070	0.0150	0.0069	0.0096
Aluminum (3A, slotted)	0.0104	0.0191	0.0101	0.0132
Nylon (1A, Not slotted)	0.0013	0.0052	0.0010	0.0025
Nylon (3A, Not slotted)	0.0026	0.0075	0.0021	0.0041
Nylon (1A, slotted)	0.0022	0.0073	0.0023	0.0039
Nylon (3A, slotted)	0.0030	0.0095	0.0029	0.0051

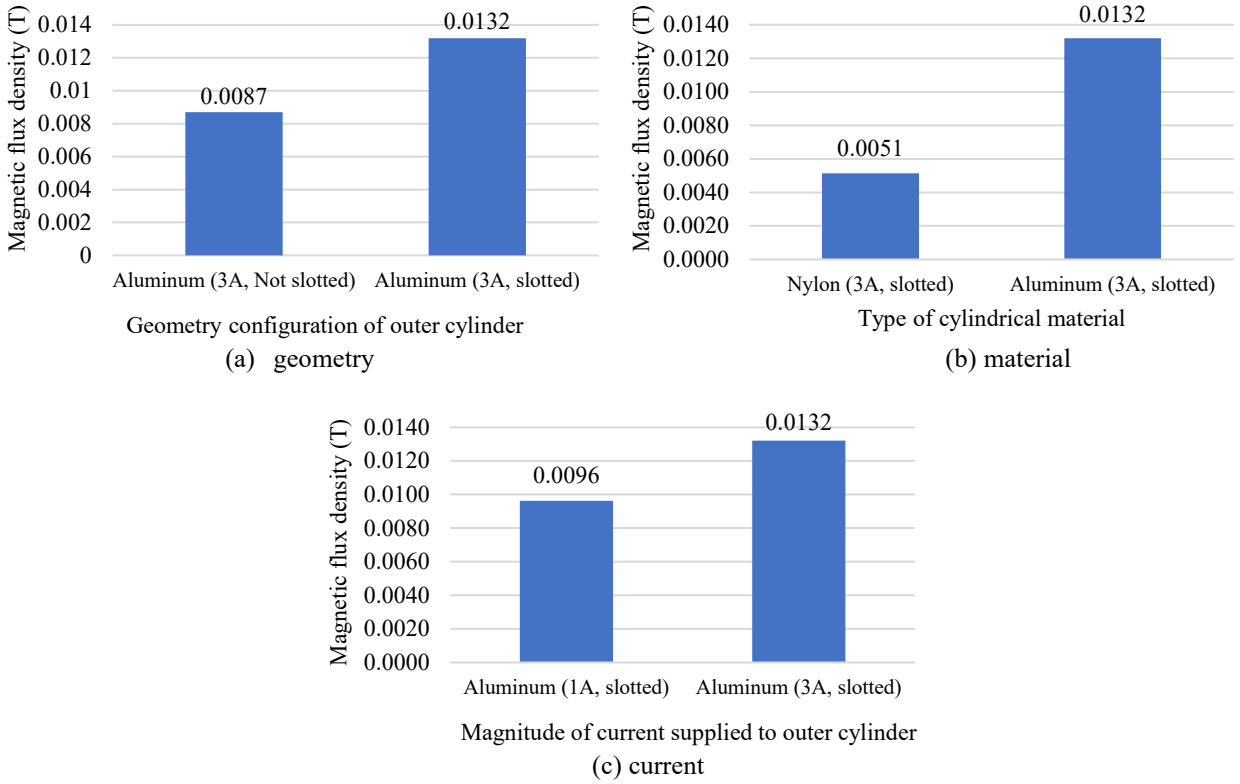

Figure 11. Parameters effect on magnetic flux density

Table 3. Experimental response data and calculation of system characteristics

Material	Geometry	No. of turns	Current supply (A)	Peak of oscillation (X)		Log decrement, δ	Damping ratio, ζ	Damping coefficient, Cd (Ns/m)
				X1	X4			
Aluminum	Non-slotted	900	1	0.0537	0.0249	0.1921	0.0306	0.5065
Aluminum	Non-slotted	900	3	0.0440	0.0188	0.2126	0.0338	0.5595
Aluminum	Slotted	900	1	0.0440	0.0086	0.4096	0.0651	1.0776
Aluminum	Slotted	900	3	0.0370	0.0025	0.6639	0.1051	1.7390
Nylon	Non-slotted	900	1	0.0541	0.0459	0.0411	0.0065	0.1083
Nylon	Non-slotted	900	3	0.0504	0.0414	0.0492	0.0830	0.1296
Nylon	Slotted	900	1	0.0580	0.0438	0.0843	0.0134	0.2218
Nylon	Slotted	900	3	0.0530	0.0352	0.1023	0.0163	0.2698

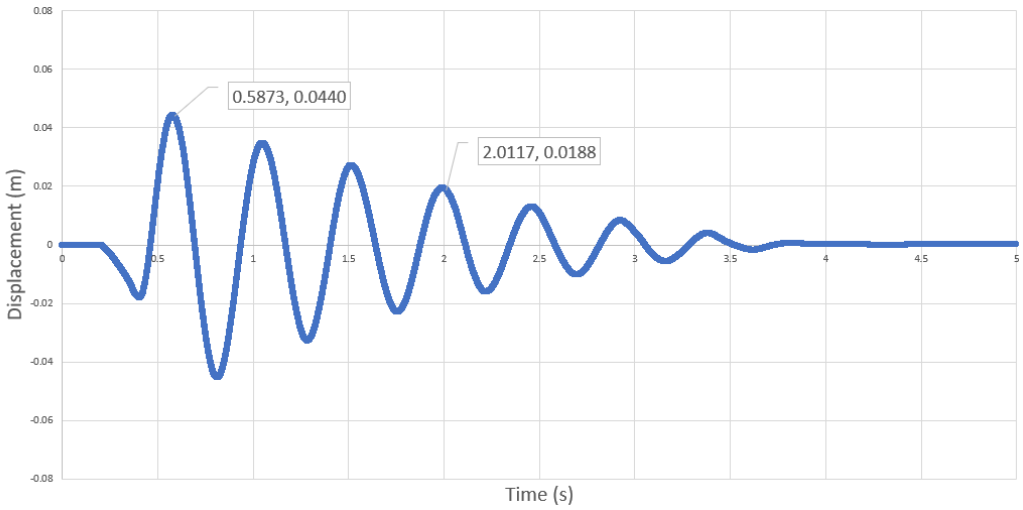

(a)

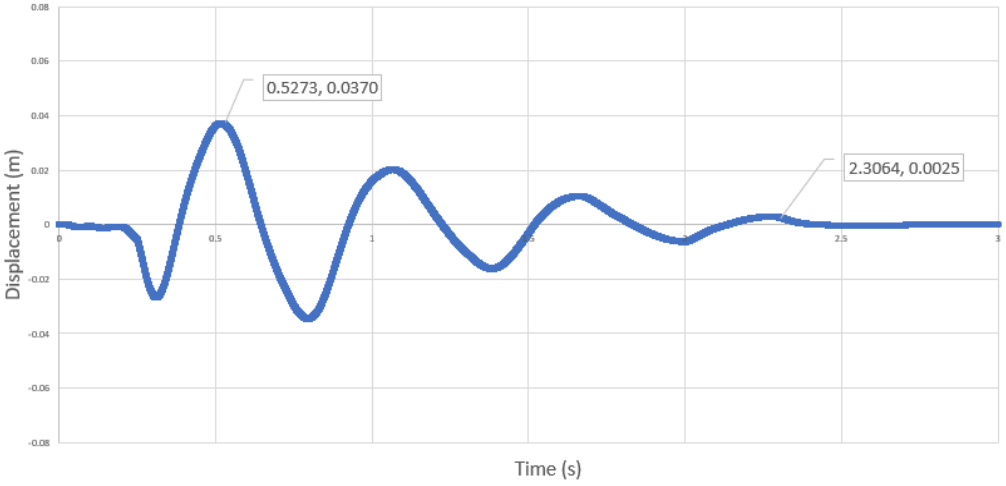

(b)

Figure 12. Graph displacement (m) against time (s) for (a) unslotted and (b) slotted aluminium damper with 3A current

4.0 DISCUSSION

From the first experimental activities, it can be shown that the magnetic flux density of the system does affect by the three parameters (material, geometry and current). Table 1 indicates the value of magnetic flux density at several locations of the wounded cylinder. An average value of the magnetic flux density calculated in the bar chart has been plotted. The results have been plotted, and a positive slope for those parameters can be seen in Figure 11. Three factors, namely material, geometry and current with two levels, have been considered in the experiment. The effect due to material shows a bigger improvement in magnetic flux values compared to the other two parameters.

The novelty of the research is endorsed by linking the vibration response of the system with the damping ecoefficiency of the overall system. The overall system has been incorporated as an electromagnetic damper, and the vibration response been analysed through the logarithmic decrement method. Thus, the damping coefficient value has been obtained by analysing the experimental results. The results can be seen in Table 3. In this experimental task, three factors with two levels of parameters have been considered. One factor that was held constant was the number of copper wire turns. The cylinder was wounded with a total of 900 turns throughout the experiment. Electromagnetic damper from aluminium with 3 Ampere current and slotted configurations shows the biggest value of damping coefficient of 1.739 Ns/m. The copper coil with 0.50 mm diameter has been wounded (900 turns) into the slotted cylindrical and is supplied with a 3 Ampere current.

Further analysis can be obtained by referring to Figure 12(a) and 12(b) where the displacement oscillation response of the system is reduced when the aluminium-slotted configuration is used. The unslotted geometry recorded around 4 seconds of settling time, while the slotted geometry settled down in 2.5 seconds. The amplitude of the response also reduced from 0.58 m to 0.53 m at the beginning of the oscillations. Vertical movement of the permanent magnet through a solenoid can create a magnetic force that can be used as a damping source in a mass spring damper. The polarity of the induced emf is such that it produces a current whose magnetic field opposes the change that produces it. The interaction between a permanent magnet and an electromagnet, created through a solenoid, results in damping due to the magnetic

repulsion between the edges of the solenoid and the magnet. There are two primary forces involved in this process. Firstly, the electromagnetic force is induced by the magnetic field within the solenoid when a current pass through the wound coils. The second force is the magnetic force generated by the reciprocating motion of the permanent magnet in the vertical direction.

4.1 Development of Empirical Model

The empirical model was obtained from the experimental result. The effect of magnetic flux density towards the damping coefficient has been plotted using Excel. From the experimental results, it can be seen that the damping coefficient Cd are positive for all values of magnetic flux density. As magnetic flux density increases, the damping coefficient Cd values grow without bound. As magnetic flux density becomes smaller approaching zero, the damping coefficient Cd values also seem to approach zero. Figure 13 shows the relation between magnetic flux density and damping coefficient, where the increase in magnetic flux increases the damping coefficient of the damping system. The regression line resembles an exponential graph ($Y= 0.069\ e^{259.4\ x}$) and has an R-squared of 92 percent. This R – squared indicated of how much strength of the relationship between the damping coefficient and magnetic flux density. The damping coefficient seems to increase exponentially with respect to the magnetic flux density. It can be observed that as the magnetic flux, B, rises, so does the damping coefficient, c. Consequently, when electromagnetic strength rises, the dampening effect on vibrations should increase.

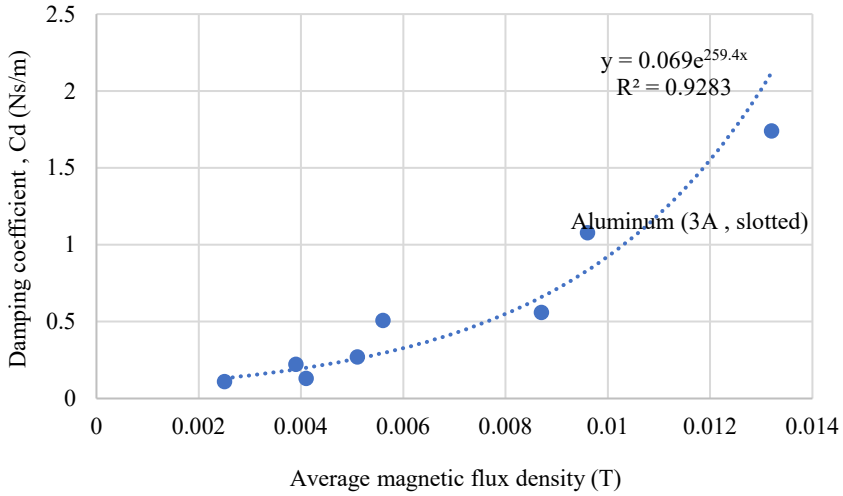

Figure 13. Graphs of maximum magnetic flux density against damping coefficient of the damping.

Initially, the data was further analysed using Minitab, where the regression analysis was performed. However, the regression equation that was plotted with respect to the damping coefficient Cd shows zero value in the predicted R-squared. This implies that the result can't fit linearly into a linear equation. Alternatively, a modification of the regression equation has been deployed by fitting the factors into the natural log equation. A basis for this modification was the result obtained through the experiment where the damping equation can be related to magnetic flux density by the exponential equation Y ($Y= 0.069\ e^{259.4\ x}$). The data has been further analysed statistically to investigate the relationship between the Cd as a response and three factors as independent variables. Inspired by the result obtained, the regression analysis was thus performed with the Cd transformed to a natural logarithm. The analysis was done by setting it as a two-sided confidence interval with a 95% confidence level for all intervals. Two levels with three factors of factorial design have been chosen in this analysis. This equation relates the damping coefficient directly to the three factors involved during the experiment; material, geometry and current. The material and geometry factors have been assigned as high' and `low' while the current supplied was taken as a numerical value (1 and 3 amperes) setting. It has been analysed as a *ln* equation which contains all three factors. This time around, the R-squared predicted value being recorded was 84.46%. The equation obtained was,

$$\ln Cd = -1.203 + 0.756\ MATERIAL + 0.319\ GEOMETRY + 0.1192\ CURRENT + 0.0549\ MATERIAL*GEOMETRY + 0.0253\ MATERIAL*CURRENT + 0.0494\ GEOMETRY*CURRENT \quad (7)$$

The fitted response of the regression equation was compared to the result obtained from the experiment, and the result has been tabulated as in Table 4. The interaction plot between the factors can be seen in Figure 14 below. Mean of response, Cd (damping coefficient) showed a positive slope which indicated that the factors do affect the response. Among all the factors, the combination of material and geometry gives the biggest slope value which implies the significance of those factors towards the damping coefficient Cd values.

Table 4. Damping coefficient value from experimental and regression analysis using Minitab

Material	Geometry	Current (Amp)	Damping coefficient from experiment using logarithmic decrement method	Regression model using MiniTab	Percentage of error (%)
Nylon	Slotted	1	0.222	0.212	-4.46
Aluminum	Slotted	3	1.739	1.663	-4.37
Aluminum	Non-Slotted	1	0.507	0.484	-4.45
Aluminum	Slotted	1	1.078	1.128	4.71
Nylon	Non-Slotted	3	0.130	0.124	-4.52
Nylon	Non-Slotted	1	0.108	0.113	4.52
Nylon	Slotted	3	0.270	0.282	4.61
Aluminum	Non-Slotted	3	0.560	0.585	4.61

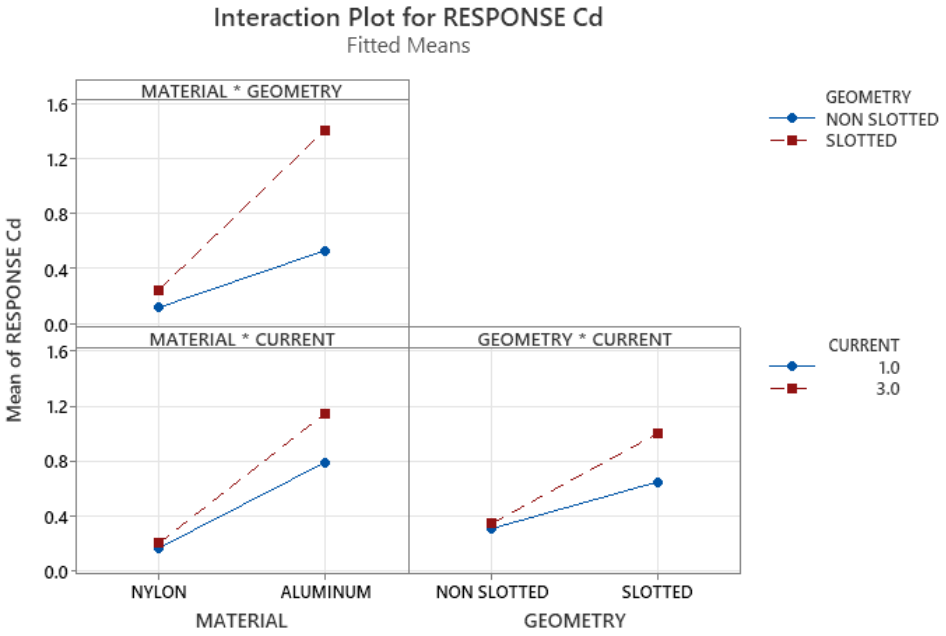

Figure 14. Interaction plot for damping coefficient factors

5.0 CONCLUSIONS

The empirical model of the damping coefficient, c of the system, has been able to drive using experimental techniques. The experiment started with several parameters (three factors, two-level) setups. The magnetic flux for each setup condition was then captured and tabulated in a table. Further analysis was done by calculating the damping coefficient, c and the data was then analysed in Minitab. The effect of geometry, material and current has been analysed using the interaction plot and the empirical model, which consisted of all parameters obtained with 84.45% of R-squared value. Two equations from the experimental using Excel and Minitab regression analysis show good similarity with only 5 percent differences. Both equations indicated magnetic field and magnetic flux of solenoid depend on the variables of the electromagnetic damper. The equations from Minitab software give a direct indication towards the parameter used (material, geometry and current). It gives the coefficient values for each factor and also any cross effect due to combinations of those factors. A regression equation shows the relation between each factor that contribute to the damping coefficient of the system. Variables of electromagnetic damper, such as types and geometry of material and current supply to the coil influences the value of vibration responses such as settling time, damping ratio, and damping coefficient.

A higher magnetic field and flux are produced when a conductor material is used. Magnetic flux and magnetic field can be increased by manipulating the material's geometry. Since slotted geometry increases the winding coil layer, it is possible to produce higher magnetic fields and fluxes of magnetism. It is possible to produce a stronger magnetic field and flux with a higher current supply as well. It is possible to reduce the settling time of oscillation by increasing damping by increasing the magnetic field and flux. An electromagnetic damper with a faster absorption rate will be more effective at reducing vibration oscillation's settling time. Furthermore, reduce unnecessary vibration delays by using damping ratios with higher values. A higher value damping coefficient means a faster return to rest. Dissipating more energy requires a higher damping coefficient and a higher damping force.

6.0 ACKNOWLEDGEMENT

The authors extend their gratitude to UPNM for providing the Research Grant of FRGS/1/2020/STG07/UPNM/03/2 and the Short-Term Research Grant (GPJP) with the code number UPNM/2016/GPJP/5/TK/5.

7.0 REFERENCES

[1] S. Li, J. Xu, X. Pu, T. Tao, H. Gao, and X. Mei, "Energy-harvesting variable/constant damping suspension system with motor based electromagnetic damper," *Energy*, vol. 189, p. 116199, 2019.

[2] H.-J.-J. Ho-Yeon Jung, In-Ho Kim, "Feasibility study of the electromagnetic damper for cable structures using real-time hybrid simulation," *Sensors*, vol. 17, no. 11, p. 2499, 2017.

[3] Q. Yang, Z. Chi, and L. Wang, "Influence and Suppression method of the Eddy current effect on the suspension system of the EMS maglev train," *Machines*, vol. 10, no. 6, pp. 1–16, 2022.

[4] T. M. Abdo, A. A. Huzayyin, A. A. Abdallah, and A. A. Adly, "Characteristics and analysis of an eddy current shock absorber damper using finite element analysis," *Actuators*, vol. 8, no. 4, 2019.

[5] N. A. Mohd Fadzil, A. M. Ishak, A. S. Abu Hasim, S. M. F. Syed Mohd Dardin, and A. A. Azid, "Power generation from wave energy using floating device," In *2018 International Conference on Electrical Engineering and Computer Science (ICECOS)*, March 2019, pp. 287–290, 2019.

[6] D. Kong, D. Jiang, and Y. Zhao, "Electromagnetic suspension acceleration measurement model and experimental analysis," *Electronics*, vol. 9, no. 2, pp. 1–13, 2020.

[7] Z. Tao *et al.*, "Theoretical model and analysis of an electromagnetic vibration energy harvester with nonlinear damping and stiffness based on 3D MEMS coils," *Journal of Physics D: Applied Physics*, vol. 53, no. 49, 2020.

[8] Abdullah, J.-H. Ahn, and H.-Y. Kim, "Effect of electromagnetic damping on system performance of voice-coil actuator applied to balancing-type scale," *Actuators*, vol. 9, no. 1, p. 8, Feb. 2020.

[9] C. W. Song and S. Y. Lee, "Design of a solenoid actuator with a magnetic plunger for miniaturised segment robots," *Applied Sciences*, vol. 5, no. 3, pp. 595–607, 2015.

[10] M. Jamshidi, C. chen Chang, and A. Bakhshi, "Design and control of a self-powered hybrid electromagnetic damper," *Journal of Sound and Vibration*, vol. 428, pp. 147–167, 2018.

[11] P. S. Zhang, "Design of electromagnetic shock absorber for energy harvesting from vehicle suspensions," M.Sc thesis, Stony Brook University, NY, USA, 2010.

[12] S. Li, J. Xu, X. Pu, T. Tao, H. Gao, and X. Mei, "Energy-harvesting variable/constant damping suspension system with motor based electromagnetic damper," *Energy*, vol. 189, no. April 2021, p. 116199, 2019.

[13] E. Diez-Jimenez, C. Alén-Cordero, R. Alcover-Sánchez, and E. Corral-Abad, "Modelling and test of an integrated magnetic spring-eddy current damper for space applications," *Actuators*, vol. 10, no. 1, pp. 1–18, 2021.

[14] P. Teli, V. Tamhankar, S. Zagade, and A. Suvre, "Study of electromagnetic damper," vol. 8, no. 09, pp. 708–711, 2019.

[15] S. G. Krishnamoorthy, I. Skiedraitė, and K. Spring, "Development of electromagnetic damper," vol. 21, no. 3, pp. 226–233, 2015.

[16] W. H. Hayt and J. A. Buck, *Engineering electromagnetics*, Eighth Edition. New York: McGraw-Hill, 2012.

[17] A. P. Zanatta, B. H. Bandeira Boff, P. R. Eckert, A. Ferreira Flores Filho, and D. G. Dorrell, "Tubular linear permanent magnet synchronous machine applied to semi-active suspension systems," *International Journal for Computation and Mathematics in Electrical and Electronic Engineering*, vol. 37, no. 5, pp. 1781–1794, Oct. 2018.

[18] W. Guo, X. Wu, X. Wei, Y. Cui, and D. Bu, "Inductance effect of passive electromagnetic dampers on building-damper system subjected to near-fault earthquakes," *Advances in Structural Engineering.*, vol. 23, no. 2, pp. 320–333, Jan. 2020.

[19] S. Suman, "Electromagnetic damping: formulas and law relate to electromagnetic damping.," 2019 [Online]. Available: https://collegedunia.com/exams/electromagnetic-damping-formulas-and-law-physics-articleid-2442 (Accessed May 25, 2022).

[20] M.F. Mohd Yusoff, A.M. Ahmad Zaidi, S.A. Firdaus Ishak, M.K. Awang, and M.F. Md Din "Simulation studies of vibration isolation using electromagnetic damper," *Jurnal Kejuruteraan UKM*, vol. 4, no. 2, pp. 119–126, 2021.

[21] E. Diez-Jimenez, R. Rizzo, M.-J. Gómez-García, and E. Corral-Abad, "Review of passive electromagnetic devices for vibration damping and isolation," *Shock and Vibration*, vol. 2019, pp. 1–16, Aug. 2019.